Article

Not peer-reviewed version

Differences in the Tumor Molecular and Microenvironmental Land-Scape Between Early (Non-metastatic) and De Novo Metastatic Primary Luminal Breast Tumors

Yentl Lambrechts , Sigrid Hatse * , François Richard , Bram Boeckx , Giuseppe Floris , Christine Desmedt , Ann Smeets , Patrick Neven , Diether Lambrechts , Hans Wildiers

Posted Date: 27 June 2023

doi: 10.20944/preprints202306.1845.v1

Keywords: (luminal) breast cancer; breast cancer biology; mutations; primary tumor; de novo - stage IV; tumor microenvironment

Article

Differences in the Tumor Molecular and Microenvironmental Land-Scape between Early (Non-Metastatic) and De Novo Metastatic Primary Luminal Breast Tumors

Yentl Lambrechts [1], Sigrid Hatse [1,*], François Richard [2], Bram Boeckx [3,4], Giuseppe Floris [5,6], Christine Desmedt [2], Ann Smeets [7,8], Patrick Neven [7], Diether Lambrechts [3,4] and Hans Wildiers [1,7]

1 Laboratory of Experimental Oncology (LEO), Department of Oncology, KU Leuven, Leuven, Belgium
2 Laboratory for Translational Breast Cancer Research (LTBCR), Department of Oncology, KU Leuven, Leuven, Belgium
3 Laboratory of Translational Genetics, Department of Human Genetics, VIB-KU Leuven, Leuven, Belgium
4 VIB Center for Cancer Biology, Leuven, Belgium
5 Laboratory for Cell and Tissue Translational Research, Department of Imaging and Radiology, KU Leuven, Leuven, Belgium
6 Department of Pathology, University Hospitals Leuven, Leuven, Belgium
7 Department of General Medical Oncology and Multidisciplinary Breast Center, University Hospitals Leuven, Leuven, Belgium
8 Department of Surgical Oncology, University Hospitals Leuven/KU Leuven, Leuven, Belgium
* Correspondence: sigrid.hatse@kuleuven.be

Simple Summary: In de novo metastatic luminal breast cancer, there remains an urgent need to fill the knowledge gap about which molecular mechanisms drive de novo metastatic disease. This study is the first to explore the transcriptomic profile and tumor microenvironmental differences at baseline of patients with ER+/HER2- de novo metastatic luminal breast cancer compared to patients with early (non-metastatic) luminal breast cancer to get a glimpse of which aspects of the tumor microenvironment of de novo luminal breast cancer are altered and to get a perspective of the molecular mechanisms underlying breast cancer metastasis.

Abstract: Background. The molecular mechanisms underlying de novo metastasis of luminal breast cancer (dnMBC) remain largely unknown. Materials & Methods. Newly diagnosed dnMBC patients (grade 2/3, ER+, PR+/-, HER2-), with available core needle biopsy (CNB), collected from the primary tumor, were selected from our clinical-pathological database. Tumors from dnMBC patients were 1:1 pairwise matched (n=32) to tumors from newly diagnosed patients who had no distant metastases at baseline (eBC group). RNA was extracted from 5 x 10µm sections of FFPE CNBs. RNA sequencing was performed using the Illumina platform. Differentially expressed genes (DEG)s were assessed using EdgeR, deconvolution was performed using CIBERSORTx to assess immune cell fractions. Paired Wilcoxon test was used to compare dnMBC and eBC groups, and corrected for false discovery rate (FDR). Results. Many regulatory DEGs were significantly downregulated in dnMBC compared to eBC. Also, immune-related and hypoxia-related signatures were significantly upregulated. Paired Wilcoxon analysis showed that *CCL17* and neutrophils fraction were significantly upregulated, whereas the memory B-cell fraction was significantly downregulated in the dnMBC group. **Conclusion.** Primary luminal tumors of dnMBC patients display significant transcriptomic and immunological differences compared to comparable tumors from eBC patients.

Keywords: (luminal) breast cancer; breast cancer biology; mutations; primary tumor; de novo – stage IV; tumor microenvironment

 doi:10.20944/preprints202306.1845.v1

Introduction

Breast cancer is the most common malignancy diagnosed in women worldwide. Improved screening programs and treatment strategies have strongly decreased breast cancer mortality rates. However, breast cancer is a heterogeneous malignancy embracing several tumor subtypes [1,2]. Hormone-sensitive luminal breast tumors, which are estrogen receptor (ER) positive, progesterone receptor (PR) positive or negative, and human epidermal growth factor receptor 2 (HER2) negative, still represent a challenging subtype for oncologists, especially the more aggressive, highly proliferative so-called luminal B-like subtype, which is associated with a poorer prognosis than the more quiescent luminal A-like. While luminal A-like breast cancer can often be adequately treated with surgical resection of the tumor and subsequent anti-hormone therapy, treatment of the luminal B-like tumor type may demand a more rigorous treatment regimen with (neo-)adjuvant systemic chemotherapy to decrease the risk of future relapse and development of distant metastasis [3–5]. Despite the advent of molecular diagnostic tests like MammaPrint® [6,7] or Oncotype Dx, which can – to some extent – predict the risk of relapse, it still remains challenging to select those patients who need chemotherapy and those who will not benefit from it.

Moreover, a subpopulation (+/- 5%) of patients with luminal B-like breast cancer presents with de novo metastatic or stage IV disease at initial diagnosis. This patient population is considered a poor prognostic group with incurable disease. De novo metastatic breast cancer (dnMBC) is managed in a different way than early (non-metastatic) breast cancer (eBC): unless there are very few and resectable metastatic lesions (also referred to as oligometastatic disease), the primary tumor is not surgically removed, and patients only receive systemic treatment. Although recurrent and de novo metastatic patients are administered comparable systemic (chemo)therapies, they differ in metastatic patterns and survival outcomes [8]. According to the majority of studies, survival rates improved over time for patients with dnMBC, whereas they did not for patients with recurrent breast cancer [9–12]. As for the metastatic patterns, Seltzer et al. reported that dnMBC has an increased frequency of PTEN, ABL2, and GATA3 mutations, together with downregulated TNFα, IL-17 signaling, and chemotaxis, as compared to recurrent metastatic breast cancer. In addition, they found an upregulation in dnMBC of steroid biosynthesis, cell migration, and cell adhesion [13].

A considerable number of individual genes (e.g., TP53, CDKN2A, PTEN, PIK3CA, RB1), microRNAs (e.g., miR-10b, miR-21, miR-200 family, and miR-29), and chemokine ligand/receptor pairs (e.g., CXCL12/CXCR4) have been linked to the metastatic process, yet the global picture remains obscure [14–16]. In particular, it is unclear which molecular mechanisms drive de novo metastatic disease: why are some tumors already metastasized at diagnosis, while other breast tumors with similar biological characteristics (size, grade, histology, receptor status, and lymph node involvement) only spread at a later stage (after initial treatment), or do not spread at all. It is also important to note that due to the limitations of standard staging procedures, de novo metastasis probably remains undetected in a significant proportion of cases at breast cancer diagnosis. Nevertheless, very few studies have investigated the biological differences between primary tumors from patients with dnMBC compared to breast tumors from patients with eBC. We have set up such a study in order to disclose the tumor molecular pathways involved and to explore potential distinct treatment options for these two patient populations. To this end, we compared the tumor transcriptomic profiles of breast tumors from patients with ER+/HER2- dnMBC and pair-wise matched breast tumors from patients with eBC.

Material and Methods

Patient population

The Leuven Multidisciplinary Breast Center (Belgium) at the University Hospitals Leuven's institutional clinicopathological database was used to select the appropriate patients. In-depth patient and tumor characteristics and follow-up data are all documented in this database.

The following inclusion criteria were used: (i) newly diagnosed between 2004 and 2019 with breast cancer, grade II or III invasive breast carcinoma of non-special type (IBC-NST) (other breast

 doi:10.20944/preprints202306.1845.v1

cancer subtypes, grade I IBC-NST, multifocal, and bilateral tumors were not allowed to avoid important population heterogeneity); (ii) tumor being ER positive and HER2 negative (ER positivity was defined as at least 1% of cells staining positive according to ASCO-CAP guidelines [17], HER-2 positivity was defined according to ASCO-CAP 2018 guidelines [18]); (iii) cTNM staging available. The staging was done according to local standards: in general, for clinical stage I-II, a chest Rx, liver ultrasound and bone scintigraphy were performed while for clinical stage III-IV, a CT or PET-CT were performed as per standard of care. CA15.3 is also routinely assessed in all new invasive breast cancer patients. In case CA15.3 was significantly increased, or suspicious lesions (potential metastases) were found on clinical examination and/or imaging, further investigations were performed to confirm de novo metastatic disease; (iv) core needle biopsy at the time of primary diagnosis available, with sufficient remaining tumor tissue (surgical resection specimens were not allowed for non-metastatic patients, to avoid technical bias) (v) no prior invasive breast cancer.

Patients with de novo metastatic disease were matched in a 1:1 fashion with patients carrying breast tumors with similar characteristics but without de novo metastases at diagnosis. Patient matching was based on age at diagnosis, tumor grade (grade 2 or grade 3), tumor size, clinical tumor staging (cT1, cT2, cT3, cT4, cT4b, cT4c, and cT4d), and lymph node involvement (cN0, cN1, cN2, and cN3). Due to the strict selection criteria and matching for multiple parameters, T/N stage could not be perfectly matched for all patient pairs, but never largely differed within patient pairs (Figure 1A).

Preprints (www.preprints.org) | NOT PEER-REVIEWED | Posted: 27 June 2023 doi:10.20944/preprints202306.1845.v1

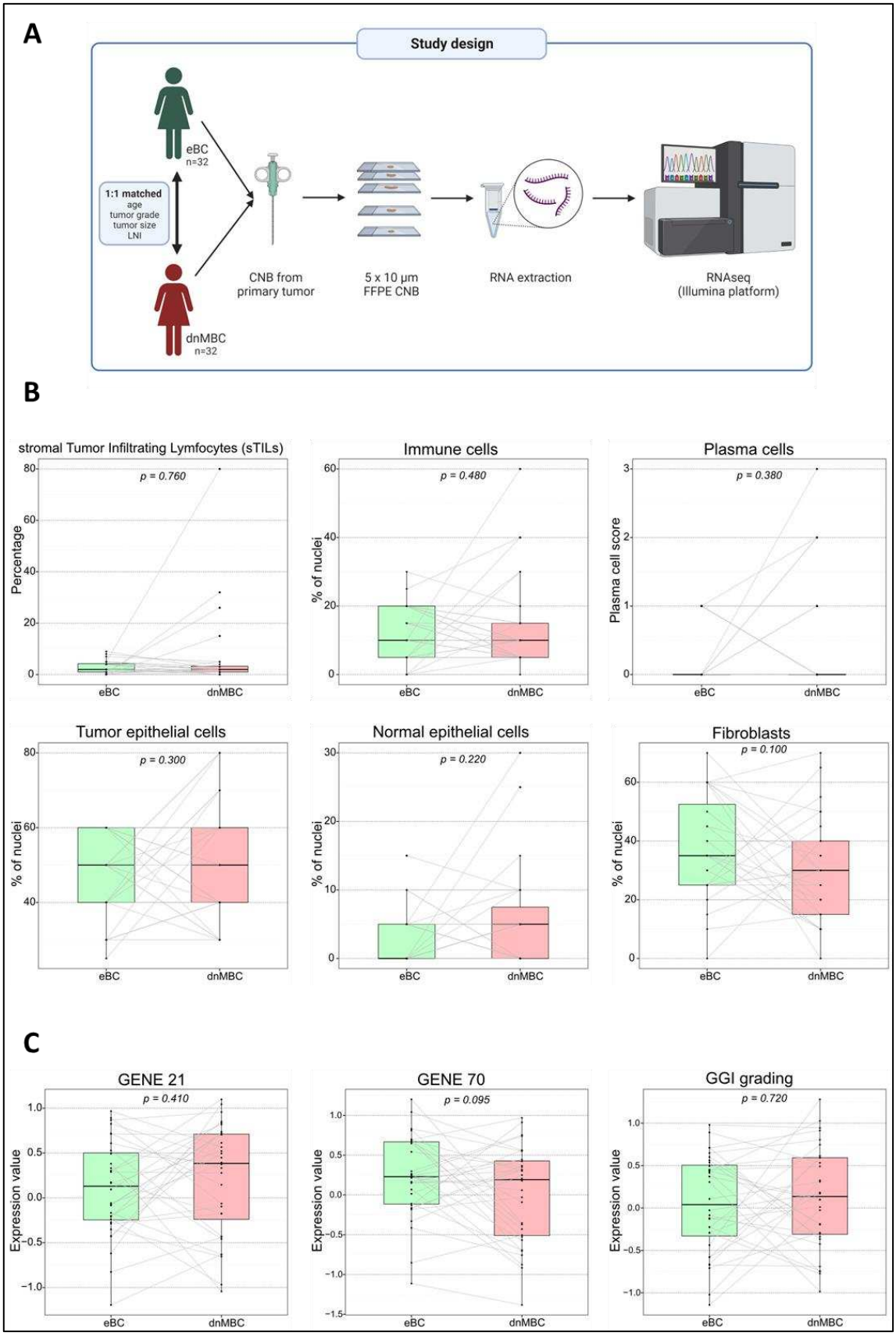

Figure 1. The study design and an overview of the comparable primary tumor CNBs based on pathology and gene expression signatures. (A) The study design includes 32 matched patients pairs (dnMBC vs. eBC), where RNA was extracted from the primary tumor CNB and sequenced using the Illumina platform. (B) The pathological parameters that were used (sTILs, immune cells, plasma cells, tumor epithelial cells, normal epithelial cells, and fibroblast) to determine of primary CNBs from both

 doi:10.20944/preprints202306.1845.v1

groups were comparable. One extra consecutive FFPE CNB slide was H&E stained and reviewed by an expert breast pathologist to ensure comparable tumor cellular composition across the entire cohort. (C). Paired Wilcoxon was used to compare gene expression profiles (GENE21, GENE70, and GGI grading) between dnMBC and eBC group. CNB: core needle biopsy; dnMBC: de novo metastatic breast cancer; eBC: non-metastatic breast cancer; FFPE: formalin-fixed paraffin-embedded; GGI: genomic grade index; sTILs: stromal tumor infiltrating lymphocytes.

Pathologic assessment of H&E-stained tumor slides and RNA extraction

RNA extraction was performed on five consecutive sections of formalin-fixed paraffin-embedded (FFPE) core needle biopsies cut at 10µm thickness and flanked by an H&E-stained slide to control representativity of the sample and the relative percentage of tumor cells, stromal components, and inflammatory infiltrate by an expert breast pathologist (GF). Shortly, the relative proportion of malignant epithelial cells, normal epithelial cells, mononuclear inflammatory cells, and fibroblast was done by eyeballing on 10x-20x magnification, scanning the whole slide, and expressing as a percentage of the total cellular (benign + malignant) population present in the sample. Additionally, the mononuclear inflammatory cells infiltrating the stroma adjacent to the tumor cells were scored using the standardized scoring method proposed by the tumor infiltrating lymphocyte (TIL)s International working group [19]. Plasma cells identified on H&E were scored using a semiquantitative grading system previously published [20]. The HighPure FFPET RNA extraction kit (Roche®) was used following the manufacturer's protocol. After extraction, RNA concentrations were measured on the NanoDrop® 2000 UV Visible Spectrophotometer (Thermo Scientific™), and quality (RNA integrity) was assessed on the Aligent Bioanalyzer.

RNA sequencing

RNA libraries were created using the Illumina TruSeq RNA sample preparation kit V2 according to the manufacturer's instructions, and resulting whole-exome libraries were sequenced on a HiSeq2500 or HiSeq4000(Illumina), generating 50-bp reads. After the removal of adaptors and optical duplicates, the raw sequencing reads were mapped to the human transcriptome GRCh37 using TopHat 2.0 and Bowtie2.0 [21]. Reads were assigned to ensemble gene IDs with the HTSeq software package. On average, $28{,}7 \times 10^6 \pm 10{,}9 \times 10^6$ reads were assigned to genes. These reads were normalized with EDASeq [21].

Bioinformatic analysis

Differential expression was assessed with EdgeR [22], and gene-set enrichment scores for the hallmark pathways were calculated with gene set variation analysis (GSVA) [23]. Gene signatures were retrieved from the literature: Gene21 [24] (proxy to Oncotype Dx), Gene70 [25] (proxy to MammaPrint), GGI grading [26], continuous hypoxia [27], cyclic hypoxia [27], IFNA [28], IFNG [28], AKT-MTOR-MG [29], and computed as a weighted average of the normalized gene expression with coefficients equals to 1 or -1 for genes positively and negatively associated with the signature, respectively.

Tests for differentially expressed genes (DEGs) were corrected for multiple testing using the Benjamini-Hochberg method. Immune cell fractions were evaluated using CIBERSORTx with 1000 permutations, in absolute mode with batch correction on normalized expression data using the signature matrix "LM22" [30]. Paired Wilcoxon test was used to compare immune-related gene signatures and cell fractions between dnMBC and eBC.

Gene ontology analysis using Gorilla [31] was performed on DEGs between eBC and dnMBC groups (p-value threshold of 10^{-3}). GO analysis was performed in the *Homo Sapiens* organism using two lists of genes (target list – DEGs; background list – all genes present within our cohort) for the three compartments (biological process, molecular function, and cellular components). Thereafter, all the significant GO terms for all three compartments were semantically summarized and visualized in the web tool REVIGO [32] using default parameters except for the species parameter set to *Homo Sapiens*.

 doi:10.20944/preprints202306.1845.v1

Results

Patient and tumor characteristics

The 1:1 matched cohort consisted of 32 patients with de novo metastasized breast cancer (dnMBC group) and 32 patients with non-metastasized early breast cancer (eBC group) with ER+ HER2- tumors. 87% (n=23) was PR+ in the dnMBC group and 94% (n=30) PR+ in the eBC group. Median ages were 62 years and 61 years for dnMBC and eBC, respectively. Most of the patients presented at diagnosis with a grade 3 tumor (dnMBC: 56% vs. eBC: 53%). Median clinical tumor size was 37mm in the dnMBC group, versus 27mm in the eBC group. When looking at the location of metastasis within the de novo metastasized group, metastasis to the bone appears to be predominant (66% of cases). All patients' characteristics are summarized in Table 1.

Table 1. Patient characteristics (age at diagnosis) and tumor properties (tumor grade and size, progesterone receptor status, lymph node involvement, and location of relapse). The matching criteria were based on age, tumor size and grade, and lymph node involvement.

Variables	Statistics	De novo metastasized BC group (dnMBC)	Non-primary metastasized BC group (eBC)
Age patients			
	N	32	32
	Median	62	61
	Average	61.69	60.84
	Range	[32.0; 88.0]	[36.0; 83.0]
Grade of tumor			
Grade 2	n/N (%)	14/32 (44%)	15/32 (47%)
Grade 3	n/N (%)	18/32 (56%)	17/32 (53%)
Progesterone receptor status			
Positive	n/N (%)	28/32 (87%)	30/32 (94%)
Negative	n/N (%)	4/32 (13%)	2/32 (6%)
Clinical staging (cT)			
cT1	n/N (%)	1/32 (3%)	6/32 (19%)
cT2	n/N (%)	17/32 (53%)	23/32 (72%)
cT3	n/N (%)	4/32 (13%)	3/32 (9%)
cT4	n/N (%)	10/32 (31%)	0/32 (0%)
cT4b	n/N (%)	3/32 (9%)	0/32 (0%)
cT4c	n/N (%)	1/32 (3%)	0/32 (0%)
cT4d	n/N (%)	5/32 (16%)	0/32 (0%)
Lymph node involvement (cN)			
cN0	n/N (%)	6/32 (19%)	21/32 (66%)
cN1	n/N (%)	11/32 (34%)	11/32 (34%)
cN2	n/N (%)	3/32 (9%)	0/32 (0%)
cN3	n/N (%)	12/32 (38%)	0/32 (0%)
Tumor size (mm)			
	Median	37	27
	Average	43.68	28.47
	Range	[16.0; 140.0]	[15.0; 55.0]
Location of metastasis			

 doi:10.20944/preprints202306.1845.v1

Brain	n/N (%)	0/32 (0%)	-
AbdominalNonLiver	n/N (%)	3/32 (9%)	-
Liver	n/N (%)	13/32 (41%)	-
Cutaneous	n/N (%)	3/32 (9%)	-
Lung	n/N (%)	11/32 (34%)	-
Bone	n/N (%)	21/32 (66%)	-
Lymph nodes	n/N (%)	12/32 (38%)	-
Others	n/N (%)	1/32 (3%)	-

De novo metastasized (dnMBC) and non-metastasized breast tumors (eBC) exhibit comparable cellular composition

Tumor cellular characteristics are indicated in Figure 1B and Supplementary Table S1. No significant differences were noted between the dnMBC group and the eBC group with regard to the presence of TILs (median: 2.0% vs. 2.0%; p=0.760), mononuclear inflammatory cells, (median: 10.0% vs. 10.0%; p=0.480), plasma cells (based on scoring, p=0.130), tumor epithelial cells (median: 50.0% vs. 50.0%; p=0.300), normal epithelial cells (median: 2.5% vs. 0.0%; p=0.220), and fibroblasts (median: 30.0% vs. 35.0%; p=0.100). These results confirm that both groups' core needle biopsies are similar in terms of cellularity and can be used for comparative transcriptomic analysis.

Gene expression profiles did not differ between de novo versus non-metastasized tumors

We have performed a paired Wilcoxon comparison of both groups for several commonly used gene expression profile signatures, such as GENE21, GENE70, and a gene expression profile from the genomic grade index (GGI). There was no significant difference between the dnMBC and the eBC tumors with regard to these gene expression signatures GENE21 (p=0.410), GENE70 (p=0.095), and GGI (p=0.720) (Figure 1C). This indicates that tumors from both groups cannot be distinguished based on the classical (e.g., proliferation-related) risk factors integrated with these prognostic tests.

Tumor microenvironment differs at the time of diagnosis

First, we looked into the GSVA hallmark signatures [23]. No hallmark signature was found statistically significant after FDR correction (Supplementary Table S2). Thereafter, we explored cell fraction changes using CIBERSORTx [30]. Lastly, we investigated differences at the individual gene level.

Hypoxia pathways are upregulated in de novo metastasized tumors. Figure 2B,C represents the integrated boxplots representing the signatures "cyclic.Hypoxia.up" and "continuous.Hypoxia.up" that were significantly more expressed in the dnMBC group, with p=0.015 and p=0.045, respectively. DEGs are depicted in the volcano plot (Figure 2A) and listed in Supplementary Table S3. Here, significant upregulation of the hypoxia-inducible factor-1 alpha (HIF-1α) in the de novo metastasized tumors is demonstrated (p<0.001). In addition, matrix metalloproteinase 2 (MMP2) (p<0.001) was upregulated in de novo metastasized compared to non-metastasized tumors. In addition, we noted an upregulation of P4HA1 (p=0.013) and PLOD2 (p=0.020) hydrolases, and a lysyl oxidase family member, such as LOX (p=0.005). Furthermore, the hypoxia-controlled gene VEGF-C, was also upregulated in the de novo metastasized tumors (p=0.021). Interestingly, the expression of ZEB1, was also significantly elevated in de novo metastasized tumors (p=0.0197). Next, we performed a gene ontology enrichment analysis from our DEGs with the online Gorilla tool, extracted the GO Terms, and inserted it in the REVIGO visualization tool. Here, we could confirm that the mechanisms involved in hypoxia, such as regulation of angiogenesis, vasculature development, ECM disassembly, endothelial cell proliferation, cell proliferation in bone marrow, and blood vessel endothelial cell migration, were involved in the de novo metastasized group (Figure 2D).

Preprints (www.preprints.org) | NOT PEER-REVIEWED | Posted: 27 June 2023 doi:10.20944/preprints202306.1845.v1

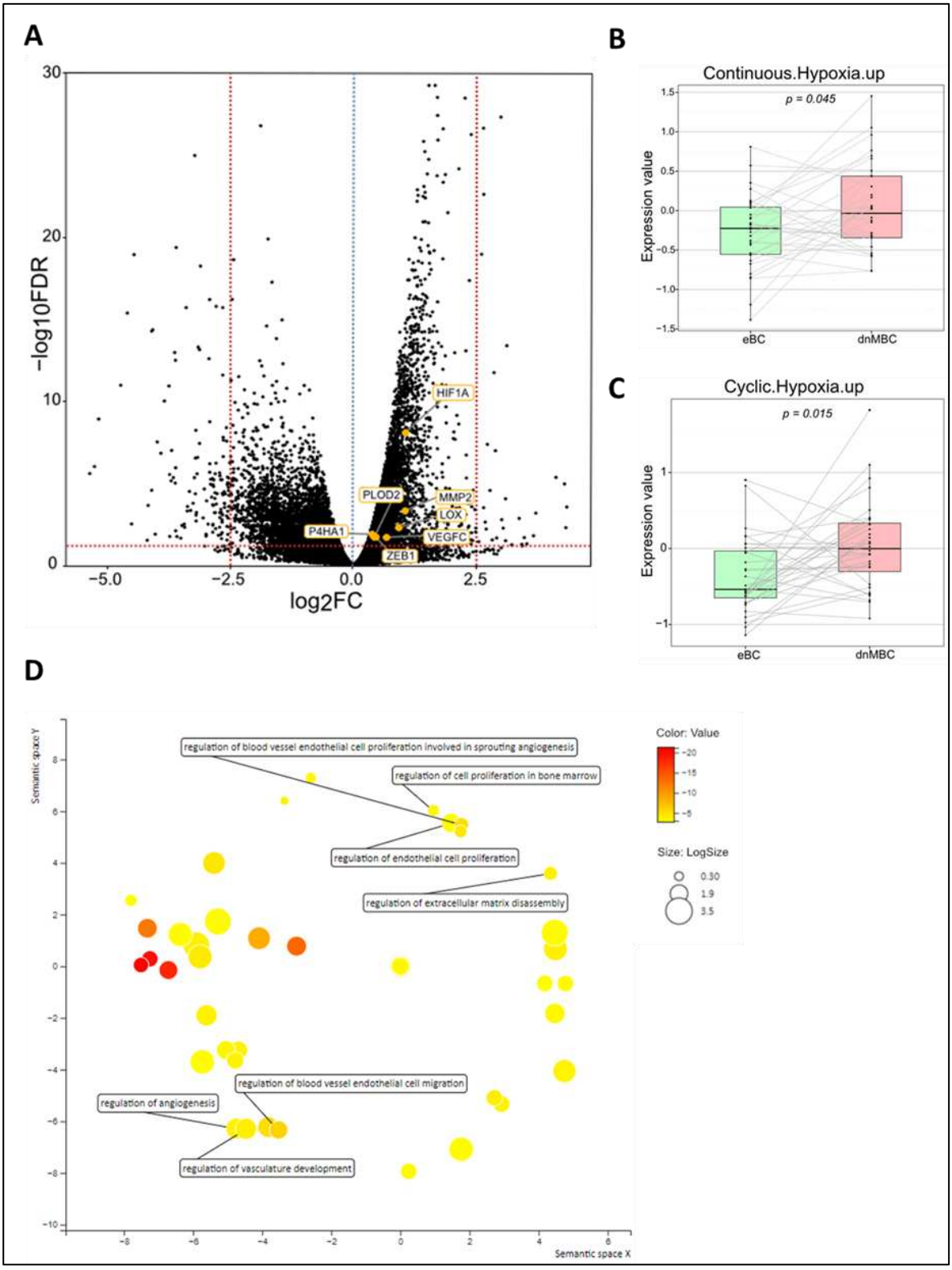

Figure 2. Transcriptomic analysis reveals that hypoxia-related pathways are upregulated in de novo metastasized tumors. (A) Volcano plot of differential expressed genes shows a statistically significant higher expression of seven hypoxia-related genes (HIF-A, PLOD2, MMP2, LOX, VEGFC, P4HA1, and ZEB1). A dotted blue line marks a $\log_2$FC value of zero. A dotted red line crossing the y-axis marks a negative $\log_{10}$FDR value of 1.3, which is the transformed FDR-corrected p-value of 0.05. A dotted red line on the x-axis marks $\log_2$FC value of 2.5 and -2.5, respectively. **(B-C)** Integrated boxplots of signatures continuous.hypoxia.up and cyclic.hypoxia.up are upregulated in the dnMBC tumor group compared to eBC tumor group. P-values are FDR-corrected. **(D)** Gene ontology enrichment analysis visualized in REVIGO displays many mechanisms that are involved in the

hypoxia pathway. The terms that are highlighted have a linkage with hypoxia only, because this REVIGO plot represents all the GO terms described in our selected significant DEG dataset. Value stand for the p-value alongside the GO term ID from our input data set. The p-values are transformed to Log10(p-value). Size stands for the Log10(number of annotations for GO Term ID in human species in the EBI GOA database). dnMBC: de novo metastasized breast tumor group; eBC: non-primary metastatic breast tumor group; FC: fold change; FDR: false discovery rate.

De novo metastasis is associated with an altered immune landscape. To investigate changes in the immune microenvironment of de novo metastasized tumors, in comparison with their non-metastasized counterparts, we first examined the signatures IFNA.down and IFNG.down, which shows an increased downregulation of these pathways in dnMBC as compared with eBC, implying a higher immune activation in dnMBC (Figure 3C–F). Paired Wilcoxon test showed a significant upregulation of both interferon signatures and of CCL17 in de novo metastasized compared to non-metastasized tumors (p=0.016, p=0.002, and p=0.050, respectively) (Figure 3B). In addition, when performing paired statistical analysis in the CIBERSORTx software, memory B-cell fraction was significantly lower (p=0.001) whereas neutrophil cell fraction was significantly higher in the de novo metastasized compared to the non-metastasized tumors (p=0.030; Figure 3D,E). Other immune cell population analyzed in the CIBERSORTx software were not significant (Supplementary Figures S4 and S5). Further elaborating on the higher neutrophil fraction in de novo metastasized tumor tissue, we investigated if the neutrophil-to-lymphocyte ratio (NLR) in blood at baseline was significantly different in dnMBC vs eBC (Supplementary Table S6). Baseline NLR was indeed higher in the dnMBC group (median=3.55, average=3.46) compared to the eBC group (median=2.55, average=3.16), but this trend did not reach statistical significance (p=0.170). In addition, we further looked into the individual DEGs (Figure 3A; Supplementary Table S7) and noticed that many chemokines were upregulated in the de novo metastasized group, such as CXCL14 (p=0.002), CXCL13 (p=0.003), CXCL11 (p=0.007), CXCL10 (p=0.049), CXCL9 (p<0.001), CXCL8 (p=0.003), CXCL2 (p=0.016), CCL19 (p=0.023), and CCL11 (p=0.023). On the other hand, several chemokine receptors were significantly downregulated in the de novo metastasized group, including CCR5 (p=0.018), CCR6 (p=0.030), and CCR10 (p=0.003). Given that many cyto/chemokines are interrelated with the downstream effects of the MAPK pathway, our results also show that the signature AKT-mTOR is upregulated in the de novo group (p=0.009; Figure 3H). Furthermore, interleukin related factors, such as IL-6 (p=0.003), IL6ST (p<0.001), ILF2 (p<0.001), IL1R1 (p<0.001), IL1R2 (p=0.025), and IL13RA1 (p<0.001) showed increased expression in de novo metastasized tumors. Interleukin signaling is closely connected to the JAK/STAT signaling pathway, of which several components were upregulated as well in the de novo metastasized group in our analysis, including *STAT1* (p=0.029), *STAT3* (p=0.001), and *JAK1* (p<0.001). In agreement with the above-mentioned CIBERSORTx findings concerning memory B cell representation in the transcriptomic profile, we found that cluster of differentiation (CD) genes that are associated with memory B cells were significantly downregulated in the de novo metastasized group, more specifically CD19 (p=0.017), CD80 (p=0.022), CD27 (p=0.025), and CD40 (p=0.004). Finally, the gene ontology enrichment analysis, visualized in REVIGO, confirmed that there is an immunity-related role in the de novo metastasized group, as reflected by the GO terms: humoral immune response, immunoglobulin production, production of molecular mediator of immune response, regulation of cytokine production involved in inflammatory response, regulation of interleukin-1 production, regulation of interleukin-1 beta production, and regulation of interleukin-6-mediated signaling pathway (Figure 3G).

Preprints (www.preprints.org) | NOT PEER-REVIEWED | Posted: 27 June 2023 doi:10.20944/preprints202306.1845.v1

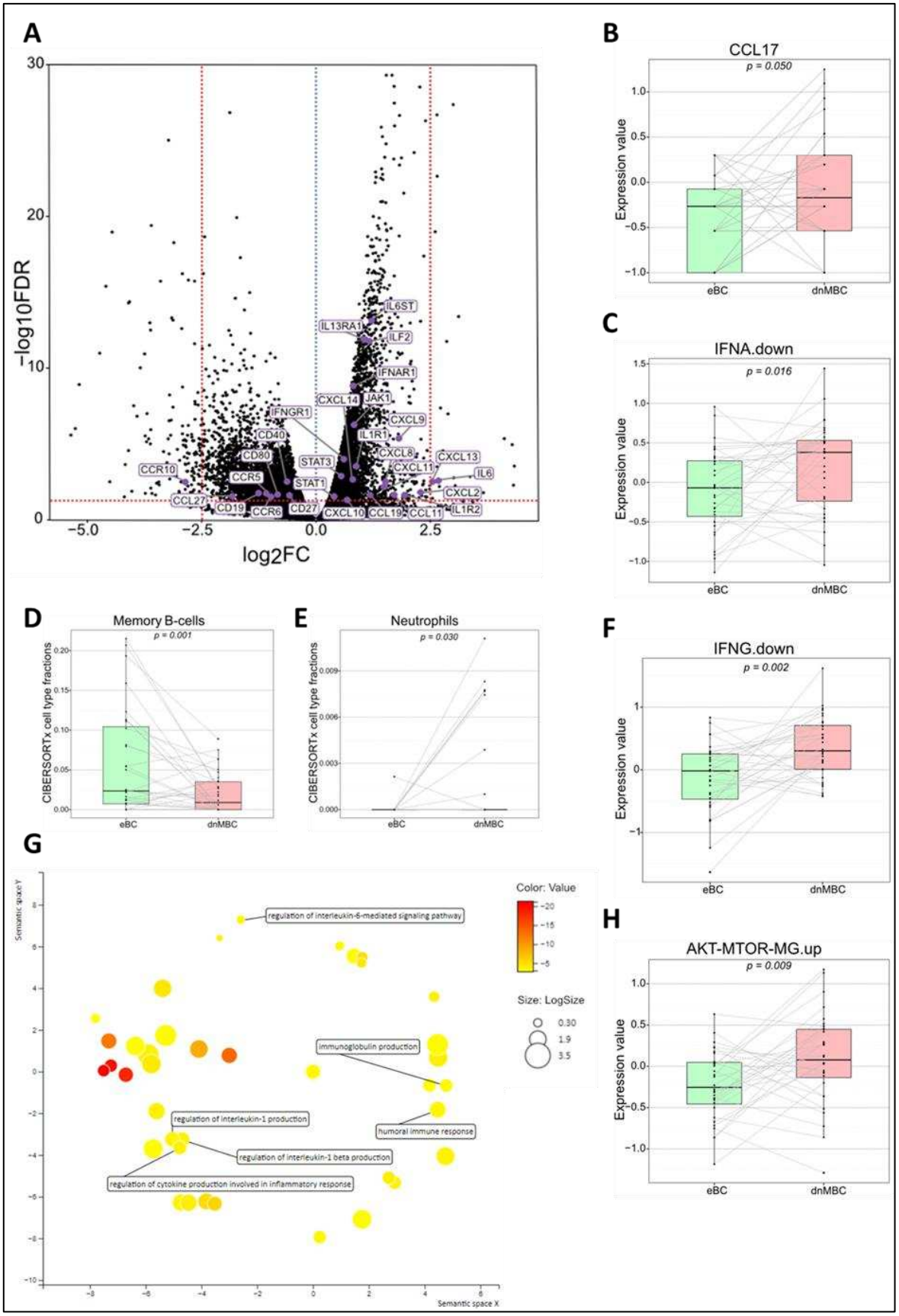

Figure 3. Transcriptomic analysis reveals that immune-related pathways are altered between both study cohorts. (A) Volcano plot of differential expressed genes shows a statistically significant upregulation of multiple chemokines and genes related to the JAK-STAT pathway, while genes of several chemokine receptors and CD-related genes of memory B-cells are significantly downregulated

 doi:10.20944/preprints202306.1845.v1

in dnMBC compared to eBC. A dotted blue line marks a log_2FC value of zero. A dotted red line crossing the y-axis marks a negative log_{10}FDR value of 1.3, which is the transformed FDR-corrected p-value of 0.05. A dotted red line on the x-axis marks log_2FC value of 2.5 and -2.5, respectively. **(B-C-F-H)** Integrated boxplots of signatures IFNA.down, IFNG.down, CCL17, and AKT-mTOR-MG.up are significantly upregulated in de novo metastasized tumors. P-values are FDR-corrected. **(D-E)** Paired Wilcoxon analysis of cell type fractions in CIBERSORTx software revealed that neutrophils were significantly upregulated, while memory B-cells were statistically significant downregulated in dnMBC vs. eBC. **(G)** Gene ontology enrichment analysis visualized in REVIGO displays many mechanisms that are involved in the immune status of the tumors. The terms that are highlighted have a linkage with immunity only, because this REVIGO plot represents all the GO terms described in our selected significant DEG dataset. Value stand for the p-value alongside the GO term ID from our input data set. The p-values are transformed to Log10(p-value). Size stands for the Log10(number of annotations for GO Term ID in human species in the EBI GOA database). dnMBC: de novo metastasized breast tumor group; eBC: non-primary metastatic breast tumor group; FC: fold change; FDR: false discovery rate.

Numerous regulatory genes are affected in the de novo metastasized tumors. Among the DEGs, as identified by their Benjamini-Hochberg value below 0.05, there were many regulatory genes, such as 14 small nucleolar RNAs (snoRNAs), 21 microRNAs, and 23 pseudogenes, which were all highly significantly downregulated in the de novo metastasized group (Figure 4A–C and Supplementary Table S8). Many aspects of the RNA regulatory compartment also emerged from the gene ontology enrichment analysis, such as miRNA-mediated gene silencing, RNA-mediated gene silencing, post-transcriptional gene silencing, regulation of translation, ncRNA-mediated, and RNA processing (Figure 4D).

Preprints (www.preprints.org) | NOT PEER-REVIEWED | Posted: 27 June 2023 doi:10.20944/preprints202306.1845.v1

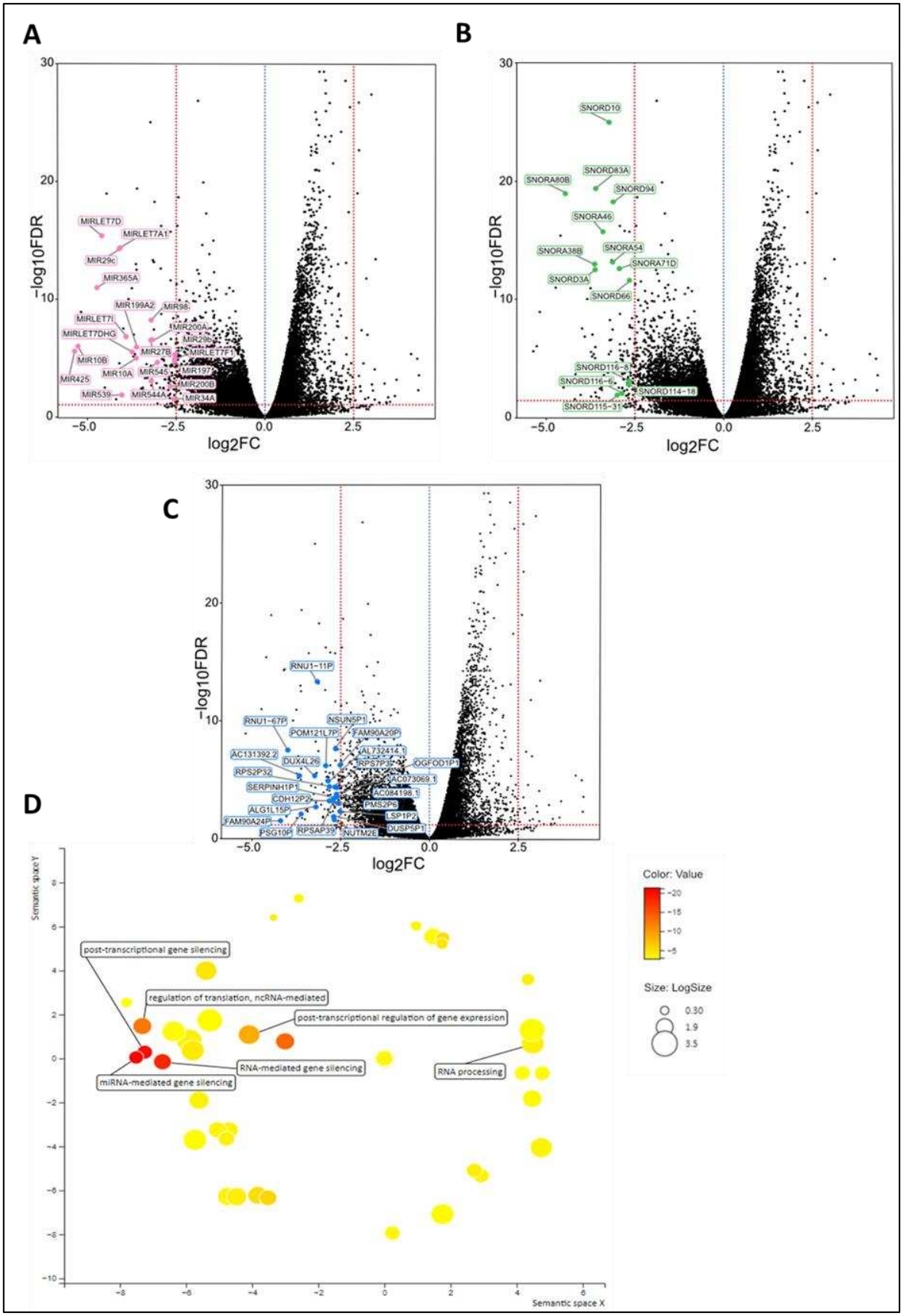

Figure 4. Regulatory genes (i.e., snoRNAs, microRNAs, and pseudogenes) are upregulated in de novo metastasized luminal breast tumors. (A-C) Volcano plot of differential expressed genes shows a statistically significant upregulation of multiple snoRNAs (n=14), microRNAs (n=21), and pseudogenes (n=23) in tumors of dnMBC compared to tumors from eBC. A dotted blue line marks a

Preprints (www.preprints.org) | NOT PEER-REVIEWED | Posted: 27 June 2023 doi:10.20944/preprints202306.1845.v1

log_2FC value of zero. A dotted red line crossing the y-axis marks a negative log_{10}FDR value of 1.3, which is the transformed FDR-corrected p-value of 0.05. A dotted red line on the x-axis marks log_2FC value of 2.5 and -2.5, respectively. (D) Gene ontology enrichment analysis visualized in REVIGO displays many gene regulatory mechanisms that are involved in the de novo tumors. The terms that are highlighted have a linkage with regulatory genes only, because this REVIGO plot represents all the GO terms described in our selected significant DEG dataset. Value stand for the p-value alongside the GO term ID from our input data set. The p-values are transformed to Log10(p-value). Size stands for the Log10(number of annotations for GO Term ID in human species in the EBI GOA database). dnMBC: de novo metastasized breast tumor group; eBC: non-primary metastatic breast tumor group; FC: fold change; FDR: false discovery rate; snoRNA: small nucleolar RNA.

Discussion

This study has investigated the difference in transcriptomic profiles of newly diagnosed de novo metastasized (dnMBC) versus non-metastasized (eBC) luminal breast tumors. Whereas no marked changes were disclosed in the classical prognostic gene expression signatures like GENE21, GENE70, and GGI, nor in the cellular composition of the tumor specimens used, the transcriptomic analysis clearly pointed to several aspects of the tumor microenvironment that are significantly altered when comparing de novo metastasized and non-metastasized tumors (Figure 5).

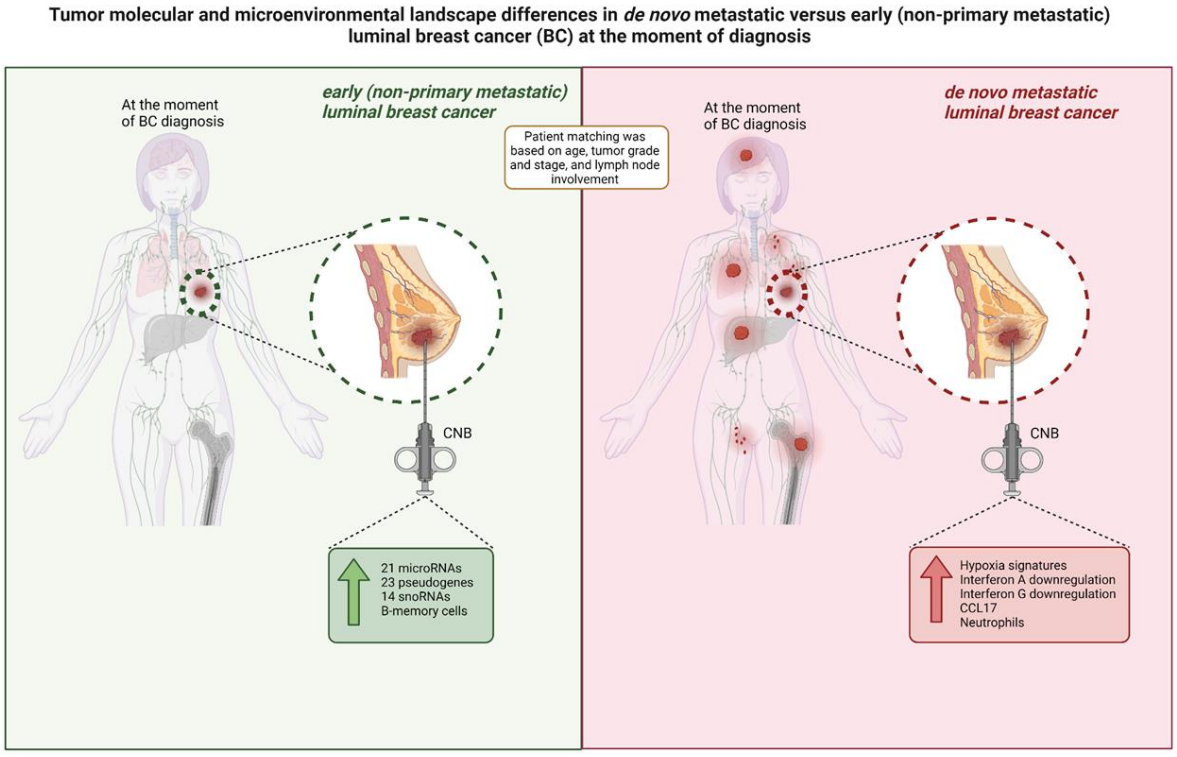

Figure 5. Overview of the tumor molecular and microenvironmental landscape differences in primary CNB tumors from luminal BC patients within our study cohort. De novo metastatic luminal BC tumors exhibit a higher expression of hypoxia signatures, immunity-related signatures (Interferon A downregulation, Interferon G downregulation, and CCL17) and neutrophils at diagnosis, while tumors from patients with non-primary metastatic luminal BC exhibit a higher expression of regulatory genes (i.e., microRNAs, pseudogenes, snoRNAs) and memory B-cells. CNB: core needle biopsy; snoRNA: small nucleolar RNA.

More specifically, we found that hypoxia is more prominent in de novo metastasized tumors compared to their non-metastasized counterparts. Hypoxia within the tumor occurs as a result of massive tumor cell proliferation and associated oxygen demand. On the other hand, oxygen availability is decreased due to the abnormal structural and functional vasculature that forms within

solid tumors [33]. Cancer cells respond to this oxygen shortage by overexpressing hypoxia-inducible factors, such as *HIF-1α*, which regulates a large number of target genes involved in invasion, extravasation, and epithelial to mesenchymal transition [34]. For instance, Gilkes and Semenza described that invasion occurs through the degradation of the ECM component by HIF-1α-dependent MMPs, like *MMP2* and *MMP9* [34]. These are endopeptidases that degrade type IV collagen, and increased levels of intra-tumoral *MMP2* were shown to be associated with poor prognosis. In addition, they described that *HIF-1 α* plays a critical role in collagen biogenesis in breast tumors by upregulating the expression of *P4HA1*, *P4HA2*, *PLOD1*, and *PLOD2* hydroxylases, as well as the lysyl oxidase family members *LOX*, *LOXL2*, and *LOXL4*. *HIF-1 α* activation modulates ECM synthesis to create a rigid microenvironment that improves cell adhesion, elongation, and motility [34,35]. In agreement with this, our study showed significant upregulation of *HIF-1α*, together with several of its target genes, including *P4HA1*, *PLOD2*, and *LOX*, in primary metastasized tumors. Besides ECM degradation, angiogenesis is also crucial for the growth and metastasis of solid tumors, such as breast tumors [34]. *HIF-1α* plays a vital role in the expression of *VEGF* under hypoxic conditions, which is also reflected in our results. Another interesting finding from our transcriptomic study is that *ZEB1* is upregulated in de novo metastatic tumors. ZEB1 is a transcriptional repressor with a potential role in initiating bone metastasis [33]. This seems consistent with the predominance of bone metastases in dnMBC patients in our study.

Secondly, we found that many immune-related genes and pathways were significantly upregulated in the dnMBC group. Chemokines and their receptors are essential in the metastatic process to direct and promote the migration of leukocytes as well as cancer cells, through the MAPK/ERK signaling pathway. We found that numerous intra-tumoral chemokines were upregulated, which can be explained by their versatile functions, including sustaining the growth and survival of tumor cells. Furthermore, we found that several chemokine receptors were downregulated in de novo metastasized tumors. When expressed by tumor cells, chemokine receptors can guide tumor cells to particular anatomic sites to form metastases, through interaction with their cognate chemokine ligands produced at distant locations. Circulating tumor cells are thus attracted into a "premetastatic niche", which provides a favorable setting for the development of metastatic tumor cells [36,37]. This mechanism has been proposed as a potential explanation for the organ-specific metastasis patterns of distinct cancer types. Chemokines also recruit different immune cell subsets into the tumor microenvironment, thus mediating the tumor immune response which may influence cancer progression [37,38]. In our study, the most significant DEG from the immunity compartment is chemokine *CXCL13*. A breast cancer study reported that overexpression of *CXCL13* in both sera and breast tumor tissues implied that CXCL13 might play a role in breast cancer initiation and progression [39,40]. Furthermore, CXCL13 is known as a B-cell-attracting chemokine (BCA-1). It was shown that a high representation of B cells in the tumor microenvironment is related to better survival in breast cancer patients [38]. We found that memory B-cells were significantly downregulated in dnMBC tumors. Memory B-cells drive the immune response because they have B-cell receptors with a high affinity that react quickly to antigen reactivation. By acting as antigen-presenting cells, they can also contribute to activating T cells [41]. Among the chemokine family, *CXCL8* also showed significant differential expression in our study. This chemokine indirectly stimulates angiogenesis by targeting and supporting the survival of vascular endothelial cells via modulation of the PI3K/MAPK pathway [38]. This signaling cascade in turn promotes downstream genes like *AKT* and *mTOR*. Accordingly, *CXCL8*, *AKT* and *mTOR* were all significantly increased in dnMBC compared to eBC in our study [42]. In addition, CXCL8 can recruit neutrophils that affect several metastasis-specific processes in the tumor, such as migration, invasion and angiogenesis [38]. Several studies have used NLR to assess the inflammatory status of a patient [43,44]. This NLR is considered a prognostic factor in cardiovascular diseases and multiple types of cancer [43,44]. In breast cancer, a meta-analysis by Wei et al. suggested that NLR is a good prognostic marker, with patients with high NLR having a poor prognosis [45]. In our study, NLR was not significantly different between dnMBC *versus* eBC patients. Furthermore, we noted that *CCL17* was significantly upregulated in de novo metastatic tumors compared to non-metastatic tumors. CCL17 is also known

as 'thymus and activation-regulated chemokine' (TARC). A murine study of hepatocellular carcinoma indicated that T-regulatory cells are attracted by CCL17 through the CCR4 axis, and that high CCR4 expression is positively associated with metastasis [46]. In addition, CCL17 seems to connect with neutrophils, as demonstrated by Mishalian and colleagues. They found that the level of CCL17 is associated with increased abundance of tumor-associated neutrophils [47]. All these findings suggest that chemokines may be tightly interconnected with the altered presence of specific immune cell subtypes in the tumor microenvironment in dnMBC tumors. Lastly, the JAK/STAT pathway seems to be involved as well in de novo metastasis seen by an upregulation of *STAT1*, *STAT3*, and *JAK1*. In addition, the interrelated interleukin signaling *IL-6* and interleukin-related factors (*IL6ST*, *ILF2*, *IL1R1*, *IL1R2*, and *IL13RA1*) were also significantly upregulated in dnMBC. Interestingly, the JAK/STAT pathway is reported to be essential for the progression/development of breast cancer bone metastases [48], which is consistent with the fact that most of the dnMBC patients in our cohort had bone metastasis at the moment of diagnosis.

Besides increased hypoxia and altered immune pathways, we also found many regulatory genes to be significantly downregulated in the de novo metastasized group. Of note, in microRNAs, the expression of microRNAs in tumor cells has been shown to be decreased by cytokines produced in the inflammatory environment of cancer. For example, in colorectal cancer cells, it has been shown that miR-34a is downregulated by the pro-inflammatory *IL-6* [49]. In addition, transforming growth factor (TGF)-β, an immune-suppressing cytokine in the microenvironment of breast cancer, inhibits members of the miR-200 family, which inhibits tumor invasion and metastatic dissemination by targeting the EMT inducing transcription factor *ZEB-1*, which is also been highlighted in the hypoxia-regulated microenvironment and bone metastasis [50,51]. MiR-200 and miR-34a are downregulated in our results which could predict that the inhibition of the EMT is lost and thus more pronounced in dnMBC tumors. In the article of Liu *et al.*, TGF-β is also linked to miR-425, a crucial suppressor of EMT and the development of TNBC through the inhibition of the TGF-β/SMAD3 signaling pathway [52]. Another EMT-suppressing microRNA is miR-29, which targets a network of pro-metastatic genes, such as *LOX*, *MMP2*, and *VEGF* [15,53]. MicroRNAs can also be involved in the MAPK/PI3K/AKT signaling pathways, as described in particular for the let-7/miR-98 family and miR-10a [51,54]. In our findings, these tumor suppressing microRNAs (miR-425, miR-29, miR-98, and miR-10a) are significantly downregulated in dnMBC tumors. Besides microRNAs, numerous snoRNAs are also downregulated in the dnMBC group. SnoRNAs play a role in the posttranscriptional modification and maturation of ribosomal RNAs (rRNAs). They consist of 60-300 nucleotides and are divided into two classes: C/D-box and H/ ACA-box snoRNAs [55]. SnoRNAs have not been extensively studied in breast tumors. In literature only few snoRNAs have been highlighted in relation to cancer, which means that extensive research is still needed in order to find out which particular role(s) they play in carcinogenesis. *SNORA38B* was reported to have a potential role in the PI3K-AKT/ERK/mTOR pathway in breast cancer [55,56]. Luo et al. found that *SNORD3A* is decreased in breast cancer as a result of the downregulation of the transcription factor Meis 1 [57]. In addition, *SNORD3A* is believed to be a competing endogenous RNA (ceRNA), by acting as a molecular sponge for microRNAs, thus regulating gene expression at posttranscriptional level [57]. In our study, the snoRNAs SNORA38B and SNORD3A were significantly downregulated in dnMBC suggesting they play a role in *de novo* breast cancer metastasis. Lastly, multiple differentially expressed regulatory genes from our study were identified as pseudogenes, i.e., non-functional copies of protein encoding genes that have been considered "junk" DNA for many years [58,59]. However, recent studies have highlighted the potential role of expressed pseudogenes in cancer progression [58]. *DUSP5P1* was found to be highly expressed in gastric cancer [60] and was linked to poor prognosis in multiple myeloma [61]. Its protein-encoding counterpart, *DUSP5*, inhibits the ERK pathway. The *DUSP5P1* pseudogene might interfere with the activity of *DUSP5*, thus perturbing ERK signaling [62]. DUSP5P1 was the only pseudogene described in literature that appeared significant our results. The other pseudogenes (n=22), all showing very highly significant differential expression between dnMBC and eBC, have not yet been studied in cancer as such, which underscores the importance and high need to profoundly investigate this type of genes in the cancer setting.

Our study has some limitations. Sample size was limited, which is mostly attributable to the fact that we applied stringent selection and matching criteria. We thought it was important to exclude rare subtypes (often with very specific biology) and only focus on IBC-NST. Matching was adequate, except for tumor size and nodal status that was a bit more advanced for the dnMBC group. This was inevitable because of insufficient number of available patients with exactly the same cT/N stage (despite having access to a database of >18.000 patients). In addition, we only used CNBs from the primary tumors, meaning that our results do not reflect the whole tumor microenvironment of luminal breast cancer.

Conclusions

This is the first study to highlight the transcriptomic and tumor microenvironmental differences of *dnMBC* as compared to eBC. Our data reveal hypoxia-related genes, immunity-related genes, microRNAs, snoRNAs, and pseudogenes seem closely related to one another in the process of primary breast cancer metastasis. Further exploration and validation in a large external cohort are necessary to understand the molecular mechanisms underlying breast cancer metastasis in de novo metastatic patients.

Supplementary Materials: Supplementary Table S1: Tumor characteristics (TILs, immune cells, tumor epithelial cells, normal epithelial cells, fibroblasts, and plasma cells) of the study cohort. Supplementary Table S2: Gene Set Variation Analysis (GSVA) between primary dnMBC tumors vs. eBC. Supplementary Table S3: Hypoxia-related DEG differences found between dnMBC and eBC tumors. Supplementary Figure S4: Integrated boxplots of paired Wilcoxon analysis of cell type fractions in the CIBERSORTx software between eBC and dnMBC group. Supplementary Figure S5: Integrated boxplots of paired Wilcoxon analysis of cell type fractions in the CIBERSORTx software between eBC and dnMBC group. Supplementary Table S6: Baseline neutrophil-to-lymphocyte ratio (NLR), neutrophil counts (percentage and absolute values), and lymphocyte counts (percentage and absolute values) of both study cohorts. Supplementary Table S7: Immunity-related DEG differences found between dnMBC and eBC tumors. Supplementary Table S8: DEG differences found in the regulatory gene category between dnMBC and eBC tumors.

Author Contributions: Conceptualization: SH – HW – YL. Data curation: BB – FR. Formal analysis: BB – FR. Funding acquisition: SH – HW – YL. Investigation: SH – YL. Methodology: SH – YL – BB – FR. Project administration: SH – YL. Resources: HW – AS – PN. Software: /. Supervision: HW – SH – YL. Validation: /. Visualization: FR – YL. Writing original draft: YL – SH – HW – GF. Writing – review & editing: All authors.

Funding: This research was supported by the Emmanuel Van der Scheuren funding from Kom op Tegen Kanker and the Translational & Clinical Research funding from Stichting tegen Kanker (Convention number: C/2020/1331). FR is funded by the FWO through a research fellowship.

Institutional Review Board Statement: This study was performed in compliance with the Helsinki Declaration and national law. The collection of patient data was approved by the ethics committee of our institution (Ethics Committee Research University Hospitals/Catholic University Leuven, study number S56919; approval number: ML10867; approval date: 12/01/2015).

Informed Consent Statement: Informed consent as obtained from all subjects involved in the study.

Data Availability Statement: The dataset used and analyzed during the current study is available from the corresponding author on reasonable request.

Acknowledgments: Not applicable.

Conflicts of Interest : The authors declare no potential conflict of interest.

References

1. Islami, F.; Ward, E.M.; Sung, H.; Cronin, K.A.; Tangka, F.K.L.; Sherman, R.L.; Zhao, J.; Anderson, R.N.; Henley, S.J.; Yabroff, K.R.; et al. Annual Report to the Nation on the Status of Cancer, Part 1: National Cancer Statistics. *J Natl Cancer Inst* **2021**, doi:10.1093/jnci/djab131.
2. Globocan 2020 Breast cancer fact sheet.

3. Bediaga, N.G.; Beristain, E.; Calvo, B.; Viguri, M.A.; Gutierrez-Corres, B.; Rezola, R.; Ruiz-Diaz, I.; Guerra, I.; de Pancorbo, M.M. Luminal B breast cancer subtype displays a dicotomic epigenetic pattern. *Springerplus* **2016**, *5*, 623, doi:10.1186/s40064-016-2235-0.
4. Ades, F.; Zardavas, D.; Bozovic-Spasojevic, I.; Pugliano, L.; Fumagalli, D.; de Azambuja, E.; Viale, G.; Sotiriou, C.; Piccart, M. Luminal B breast cancer: molecular characterization, clinical management, and future perspectives. *J Clin Oncol* **2014**, *32*, 2794-2803, doi:10.1200/JCO.2013.54.1870.
5. Li, Z.H.; Hu, P.H.; Tu, J.H.; Yu, N.S. Luminal B breast cancer: patterns of recurrence and clinical outcome. *Oncotarget* **2016**, *7*, 65024-65033, doi:10.18632/oncotarget.11344.
6. Audeh, W.; Blumencranz, L.; Kling, H.; Trivedi, H.; Srkalovic, G. Prospective Validation of a Genomic Assay in Breast Cancer: The 70-gene MammaPrint Assay and the MINDACT Trial. *Acta Med Acad* **2019**, *48*, 18-34, doi:10.5644/ama2006-124.239.
7. Piccart, M.; van 't Veer, L.J.; Poncet, C.; Lopes Cardozo, J.M.N.; Delaloge, S.; Pierga, J.Y.; Vuylsteke, P.; Brain, E.; Vrijaldenhoven, S.; Neijenhuis, P.A.; et al. 70-gene signature as an aid for treatment decisions in early breast cancer: updated results of the phase 3 randomised MINDACT trial with an exploratory analysis by age. *Lancet Oncol* **2021**, *22*, 476-488, doi:10.1016/S1470-2045(21)00007-3.
8. Gennari, A.; Andre, F.; Barrios, C.H.; Cortes, J.; de Azambuja, E.; DeMichele, A.; Dent, R.; Fenlon, D.; Gligorov, J.; Hurvitz, S.A.; et al. ESMO Clinical Practice Guideline for the diagnosis, staging and treatment of patients with metastatic breast cancer. *Ann Oncol* **2021**, *32*, 1475-1495, doi:10.1016/j.annonc.2021.09.019.
9. McKenzie, H.S.; Maishman, T.; Simmonds, P.; Durcan, L.; Group, P.S.; Eccles, D.; Copson, E. Survival and disease characteristics of de novo versus recurrent metastatic breast cancer in a cohort of young patients. *Br J Cancer* **2020**, *122*, 1618-1629, doi:10.1038/s41416-020-0784-z.
10. Yamamura, J.; Kamigaki, S.; Fujita, J.; Osato, H.; Komoike, Y. The Difference in Prognostic Outcomes Between De Novo Stage IV and Recurrent Metastatic Patients with Hormone Receptor-positive, HER2-negative Breast Cancer. In Vivo **2018**, *32*, 353-358, doi:10.21873/invivo.11245.
11. Malmgren, J.A.; Mayer, M.; Atwood, M.K.; Kaplan, H.G. Differential presentation and survival of de novo and recurrent metastatic breast cancer over time: 1990-2010. *Breast Cancer Res Treat* **2018**, *167*, 579-590, doi:10.1007/s10549-017-4529-5.
12. Lord, S.J.; Bahlmann, K.; O'Connell, D.L.; Kiely, B.E.; Daniels, B.; Pearson, S.A.; Beith, J.; Bulsara, M.K.; Houssami, N. De novo and recurrent metastatic breast cancer - A systematic review of population-level changes in survival since 1995. *EClinicalMedicine* **2022**, *44*, 101282, doi:10.1016/j.eclinm.2022.101282.
13. Seltzer, S.; Corrigan, M.; O'Reilly, S. The clinicomolecular landscape of de novo versus relapsed stage IV metastatic breast cancer. *Exp Mol Pathol* **2020**, *114*, 104404, doi:10.1016/j.yexmp.2020.104404.
14. Fares, J.; Fares, M.Y.; Khachfe, H.H.; Salhab, H.A.; Fares, Y. Molecular principles of metastasis: a hallmark of cancer revisited. *Signal Transduct Target Ther* **2020**, *5*, 28, doi:10.1038/s41392-020-0134-x.
15. Petri, B.J.; Klinge, C.M. Regulation of breast cancer metastasis signaling by miRNAs. *Cancer Metastasis Rev* **2020**, *39*, 837-886, doi:10.1007/s10555-020-09905-7.
16. Marcuzzi, E.; Angioni, R.; Molon, B.; Cali, B. Chemokines and Chemokine Receptors: Orchestrating Tumor Metastasization. *Int J Mol Sci* **2018**, *20*, doi:10.3390/ijms20010096.
17. Allison, K.H.; Hammond, M.E.H.; Dowsett, M.; McKernin, S.E.; Carey, L.A.; Fitzgibbons, P.L.; Hayes, D.F.; Lakhani, S.R.; Chavez-MacGregor, M.; Perlmutter, J.; et al. Estrogen and Progesterone Receptor Testing in Breast Cancer: American Society of Clinical Oncology/College of American Pathologists Guideline Update. *Arch Pathol Lab Med* **2020**, *144*, 545-563, doi:10.5858/arpa.2019-0904-SA.
18. Wolff, A.C.; Hammond, M.E.H.; Allison, K.H.; Harvey, B.E.; Mangu, P.B.; Bartlett, J.M.S.; Bilous, M.; Ellis, I.O.; Fitzgibbons, P.; Hanna, W.; et al. Human Epidermal Growth Factor Receptor 2 Testing in Breast Cancer: American Society of Clinical Oncology/College of American Pathologists Clinical Practice Guideline Focused Update. *J Clin Oncol* **2018**, *36*, 2105-2122, doi:10.1200/JCO.2018.77.8738.
19. Hendry, S.; Salgado, R.; Gevaert, T.; Russell, P.A.; John, T.; Thapa, B.; Christie, M.; van de Vijver, K.; Estrada, M.V.; Gonzalez-Ericsson, P.I.; et al. Assessing Tumor-infiltrating Lymphocytes in Solid Tumors: A Practical Review for Pathologists and Proposal for a Standardized Method From the International Immunooncology Biomarkers Working Group: Part 1: Assessing the Host Immune Response, TILs in Invasive Breast Carcinoma and Ductal Carcinoma In Situ, Metastatic Tumor Deposits and Areas for Further Research. *Adv Anat Pathol* **2017**, *24*, 235-251, doi:10.1097/PAP.0000000000000162.
20. Deman, F.; Punie, K.; Laenen, A.; Neven, P.; Oldenburger, E.; Smeets, A.; Nevelsteen, I.; Van Ongeval, C.; Baten, A.; Faes, T.; et al. Assessment of stromal tumor infiltrating lymphocytes and immunohistochemical

features in invasive micropapillary breast carcinoma with long-term outcomes. *Breast Cancer Res Treat* **2020**, *184*, 985-998, doi:10.1007/s10549-020-05913-x.

21. Risso, D.; Schwartz, K.; Sherlock, G.; Dudoit, S. GC-content normalization for RNA-Seq data. *BMC Bioinformatics* **2011**, *12*, 480, doi:10.1186/1471-2105-12-480.
22. Chen, Y.; Lun, A.T.; Smyth, G.K. From reads to genes to pathways: differential expression analysis of RNA-Seq experiments using Rsubread and the edgeR quasi-likelihood pipeline. *F1000Res* **2016**, *5*, 1438, doi:10.12688/f1000research.8987.2.
23. Subramanian, A.; Tamayo, P.; Mootha, V.K.; Mukherjee, S.; Ebert, B.L.; Gillette, M.A.; Paulovich, A.; Pomeroy, S.L.; Golub, T.R.; Lander, E.S.; et al. Gene set enrichment analysis: a knowledge-based approach for interpreting genome-wide expression profiles. *Proc Natl Acad Sci U S A* **2005**, *102*, 15545-15550, doi:10.1073/pnas.0506580102.
24. Paik, S.; Shak, S.; Tang, G.; Kim, C.; Baker, J.; Cronin, M.; Baehner, F.L.; Walker, M.G.; Watson, D.; Park, T.; et al. A multigene assay to predict recurrence of tamoxifen-treated, node-negative breast cancer. *N Engl J Med* **2004**, *351*, 2817-2826, doi:10.1056/NEJMoa041588.
25. van 't Veer, L.J.; Dai, H.; van de Vijver, M.J.; He, Y.D.; Hart, A.A.; Mao, M.; Peterse, H.L.; van der Kooy, K.; Marton, M.J.; Witteveen, A.T.; et al. Gene expression profiling predicts clinical outcome of breast cancer. *Nature* **2002**, *415*, 530-536, doi:10.1038/415530a.
26. Sotiriou, C.; Wirapati, P.; Loi, S.; Harris, A.; Fox, S.; Smeds, J.; Nordgren, H.; Farmer, P.; Praz, V.; Haibe-Kains, B.; et al. Gene expression profiling in breast cancer: understanding the molecular basis of histologic grade to improve prognosis. *J Natl Cancer Inst* **2006**, *98*, 262-272, doi:10.1093/jnci/djj052.
27. Boidot, R.; Branders, S.; Helleputte, T.; Rubio, L.I.; Dupont, P.; Feron, O. A generic cycling hypoxia-derived prognostic gene signature: application to breast cancer profiling. *Oncotarget* **2014**, *5*, 6947-6963, doi:10.18632/oncotarget.2285.
28. Der, S.D.; Zhou, A.; Williams, B.R.; Silverman, R.H. Identification of genes differentially regulated by interferon alpha, beta, or gamma using oligonucleotide arrays. *Proc Natl Acad Sci U S A* **1998**, *95*, 15623-15628, doi:10.1073/pnas.95.26.15623.
29. Majumder, P.K.; Febbo, P.G.; Bikoff, R.; Berger, R.; Xue, Q.; McMahon, L.M.; Manola, J.; Brugarolas, J.; McDonnell, T.J.; Golub, T.R.; et al. mTOR inhibition reverses Akt-dependent prostate intraepithelial neoplasia through regulation of apoptotic and HIF-1-dependent pathways. *Nat Med* **2004**, *10*, 594-601, doi:10.1038/nm1052.
30. Newman, A.M.; Steen, C.B.; Liu, C.L.; Gentles, A.J.; Chaudhuri, A.A.; Scherer, F.; Khodadoust, M.S.; Esfahani, M.S.; Luca, B.A.; Steiner, D.; et al. Determining cell type abundance and expression from bulk tissues with digital cytometry. *Nat Biotechnol* **2019**, *37*, 773-782, doi:10.1038/s41587-019-0114-2.
31. Eden, E.; Navon, R.; Steinfeld, I.; Lipson, D.; Yakhini, Z. GOrilla: a tool for discovery and visualization of enriched GO terms in ranked gene lists. *BMC Bioinformatics* **2009**, *10*, 48, doi:10.1186/1471-2105-10-48.
32. Supek, F.; Bosnjak, M.; Skunca, N.; Smuc, T. REVIGO summarizes and visualizes long lists of gene ontology terms. *PLoS One* **2011**, *6*, e21800, doi:10.1371/journal.pone.0021800.
33. Gilkes, D.M. Implications of Hypoxia in Breast Cancer Metastasis to Bone. *Int J Mol Sci* **2016**, *17*, doi:10.3390/ijms17101669.
34. Gilkes, D.M.; Semenza, G.L. Role of hypoxia-inducible factors in breast cancer metastasis. *Future Oncol* **2013**, *9*, 1623-1636, doi:10.2217/fon.13.92.
35. Gilkes, D.M.; Bajpai, S.; Chaturvedi, P.; Wirtz, D.; Semenza, G.L. Hypoxia-inducible factor 1 (HIF-1) promotes extracellular matrix remodeling under hypoxic conditions by inducing P4HA1, P4HA2, and PLOD2 expression in fibroblasts. *J Biol Chem* **2013**, *288*, 10819-10829, doi:10.1074/jbc.M112.442939.
36. Chow, M.T.; Luster, A.D. Chemokines in cancer. *Cancer Immunol Res* **2014**, *2*, 1125-1131, doi:10.1158/2326-6066.CIR-14-0160.
37. Balkwill, F. Cancer and the chemokine network. *Nat Rev Cancer* **2004**, *4*, 540-550, doi:10.1038/nrc1388.
38. Nagarsheth, N.; Wicha, M.S.; Zou, W. Chemokines in the cancer microenvironment and their relevance in cancer immunotherapy. *Nat Rev Immunol* **2017**, *17*, 559-572, doi:10.1038/nri.2017.49.
39. Panse, J.; Friedrichs, K.; Marx, A.; Hildebrandt, Y.; Luetkens, T.; Barrels, K.; Horn, C.; Stahl, T.; Cao, Y.; Milde-Langosch, K.; et al. Chemokine CXCL13 is overexpressed in the tumour tissue and in the peripheral blood of breast cancer patients. *Br J Cancer* **2008**, *99*, 930-938, doi:10.1038/sj.bjc.6604621.
40. Jiang, L.; Wang, D.; Sheng, M.; Tong, D.; Liu, H.; Dong, L.; Ma, J. CXCL13/CXCR5 are potential biomarkers for diagnosis and prognosis for breast cancer. *J BUON* **2020**, *25*, 2552-2561.

41. Downs-Canner, S.M.; Meier, J.; Vincent, B.G.; Serody, J.S. B Cell Function in the Tumor Microenvironment. *Annu Rev Immunol* **2022**, *40*, 169-193, doi:10.1146/annurev-immunol-101220-015603.
42. Asokan, S.; Bandapalli, O.R. CXCL8 Signaling in the Tumor Microenvironment. *Adv Exp Med Biol* **2021**, *1302*, 25-39, doi:10.1007/978-3-030-62658-7_3.
43. Howard, R.; Kanetsky, P.A.; Egan, K.M. Exploring the prognostic value of the neutrophil-to-lymphocyte ratio in cancer. *Sci Rep* **2019**, *9*, 19673, doi:10.1038/s41598-019-56218-z.
44. Forget, P.; Khalifa, C.; Defour, J.P.; Latinne, D.; Van Pel, M.C.; De Kock, M. What is the normal value of the neutrophil-to-lymphocyte ratio? *BMC Res Notes* **2017**, *10*, 12, doi:10.1186/s13104-016-2335-5.
45. Wei, B.; Yao, M.; Xing, C.; Wang, W.; Yao, J.; Hong, Y.; Liu, Y.; Fu, P. The neutrophil lymphocyte ratio is associated with breast cancer prognosis: an updated systematic review and meta-analysis. *Onco Targets Ther* **2016**, *9*, 5567-5575, doi:10.2147/OTT.S108419.
46. Zhou, S.L.; Zhou, Z.J.; Hu, Z.Q.; Huang, X.W.; Wang, Z.; Chen, E.B.; Fan, J.; Cao, Y.; Dai, Z.; Zhou, J. Tumor-Associated Neutrophils Recruit Macrophages and T-Regulatory Cells to Promote Progression of Hepatocellular Carcinoma and Resistance to Sorafenib. *Gastroenterology* **2016**, *150*, 1646-1658 e1617, doi:10.1053/j.gastro.2016.02.040.
47. Mishalian, I.; Bayuh, R.; Eruslanov, E.; Michaeli, J.; Levy, L.; Zolotarov, L.; Singhal, S.; Albelda, S.M.; Granot, Z.; Fridlender, Z.G. Neutrophils recruit regulatory T-cells into tumors via secretion of CCL17--a new mechanism of impaired antitumor immunity. *Int J Cancer* **2014**, *135*, 1178-1186, doi:10.1002/ijc.28770.
48. Song, X.; Wei, C.; Li, X. The Signaling Pathways Associated With Breast Cancer Bone Metastasis. *Front Oncol* **2022**, *12*, 855609, doi:10.3389/fonc.2022.855609.
49. Yang, S.; Li, Y.; Gao, J.; Zhang, T.; Li, S.; Luo, A.; Chen, H.; Ding, F.; Wang, X.; Liu, Z. MicroRNA-34 suppresses breast cancer invasion and metastasis by directly targeting Fra-1. *Oncogene* **2013**, *32*, 4294-4303, doi:10.1038/onc.2012.432.
50. Gregory, P.A.; Bert, A.G.; Paterson, E.L.; Barry, S.C.; Tsykin, A.; Farshid, G.; Vadas, M.A.; Khew-Goodall, Y.; Goodall, G.J. The miR-200 family and miR-205 regulate epithelial to mesenchymal transition by targeting ZEB1 and SIP1. *Nat Cell Biol* **2008**, *10*, 593-601, doi:10.1038/ncb1722.
51. Lin, X.; Chen, L.; Yao, Y.; Zhao, R.; Cui, X.; Chen, J.; Hou, K.; Zhang, M.; Su, F.; Chen, J.; et al. CCL18-mediated down-regulation of miR98 and miR27b promotes breast cancer metastasis. *Oncotarget* **2015**, *6*, 20485-20499, doi:10.18632/oncotarget.4107.
52. Liu, Y.; Chen, J. miR-425 suppresses EMT and the development of TNBC (triple-negative breast cancer) by targeting the TGF-beta 1/SMAD 3 signaling pathway. *RSC Adv* **2018**, *9*, 151-165, doi:10.1039/c8ra08872a.
53. Wang, Y.; Zhang, X.; Li, H.; Yu, J.; Ren, X. The role of miRNA-29 family in cancer. *Eur J Cell Biol* **2013**, *92*, 123-128, doi:10.1016/j.ejcb.2012.11.004.
54. Ke, K.; Lou, T. MicroRNA-10a suppresses breast cancer progression via PI3K/Akt/mTOR pathway. *Oncol Lett* **2017**, *14*, 5994-6000, doi:10.3892/ol.2017.6930.
55. Zhuo, Y.; Li, S.; Hu, W.; Zhang, Y.; Shi, Y.; Zhang, F.; Zhang, J.; Wang, J.; Liao, M.; Chen, J.; et al. Targeting SNORA38B attenuates tumorigenesis and sensitizes immune checkpoint blockade in non-small cell lung cancer by remodeling the tumor microenvironment via regulation of GAB2/AKT/mTOR signaling pathway. *J Immunother Cancer* **2022**, *10*, doi:10.1136/jitc-2021-004113.
56. Adams, S.J.; Aydin, I.T.; Celebi, J.T. GAB2--a scaffolding protein in cancer. *Mol Cancer Res* **2012**, *10*, 1265-1270, doi:10.1158/1541-7786.MCR-12-0352.
57. Luo, L.; Zhang, J.; Tang, H.; Zhai, D.; Huang, D.; Ling, L.; Wang, X.; Liu, T.; Zhang, Q.; Zhang, Z.; et al. LncRNA SNORD3A specifically sensitizes breast cancer cells to 5-FU by sponging miR-185-5p to enhance UMPS expression. *Cell Death Dis* **2020**, *11*, 329, doi:10.1038/s41419-020-2557-2.
58. Sisu, C. Pseudogenes as Biomarkers and Therapeutic Targets in Human Cancers. *Methods Mol Biol* **2021**, *2324*, 319-337, doi:10.1007/978-1-0716-1503-4_20.
59. Salmena, L. Pseudogenes: Four Decades of Discovery. *Methods Mol Biol* **2021**, *2324*, 3-18, doi:10.1007/978-1-0716-1503-4_1.
60. Wang, X.; Zhang, L.; Liang, Q.; Wong, C.C.; Chen, H.; Gou, H.; Dong, Y.; Liu, W.; Li, Z.; Ji, J.; et al. DUSP5P1 promotes gastric cancer metastasis and platinum drug resistance. *Oncogenesis* **2022**, *11*, 66, doi:10.1038/s41389-022-00441-3.
61. Zhou, L.Y.; Yin, J.Y.; Tang, Q.; Zhai, L.L.; Zhang, T.J.; Wang, Y.X.; Yang, D.Q.; Qian, J.; Lin, J.; Deng, Z.Q. High expression of dual-specificity phosphatase 5 pseudogene 1 (DUSP5P1) is associated with poor prognosis in acute myeloid leukemia. *Int J Clin Exp Pathol* **2015**, *8*, 16073-16080.

62. Staege, M.S.; Muller, K.; Kewitz, S.; Volkmer, I.; Mauz-Korholz, C.; Bernig, T.; Korholz, D. Expression of dual-specificity phosphatase 5 pseudogene 1 (DUSP5P1) in tumor cells. *PLoS One* **2014**, *9*, e89577, doi:10.1371/journal.pone.0089577.